



Spatial analysis of selected soil attributes across an alpine topographic/snow gradient

M. Iggy Litaor^{1,*}, T.R. Seastedt² and D.A. Walker³

¹Department of Biotechnology and Environmental Sciences, Tel-Hai Academic College, Upper Galilee, 12210, Israel; ²University of Colorado, EPOB, and INSTAAR, Boulder, Colorado 80309-0450, USA; ³University of Alaska, Fairbanks, Fairbanks, AK 99775-7000, USA; *Author for correspondence (e-mail: litaori@telhai.ac.il)

Received 1 March 2000; accepted in revised form 8 October 2001

Key words: Alpine landscape, Colorado, Fractal analysis, Geostatistical modeling, Rocky mountains

Abstract

The impact of the topographic/snow gradient on soil processes in alpine tundra on Niwot Ridge of the Colorado Front Range (Rocky mts, USA) was assessed using geostatistical modeling and a fractal approach. The mean snow depth, which measured between 1984 and 2000, exhibited a smooth spatial continuity across the study grid area (550 × 400 meter). Soil color variables showed a nested structure that was attributed to a confounded effect of various soil-forming factors on catenary processes. The spatial structure of texture classes exhibited no spatial structure and was explained by data sparsity, cryoturbation, and biological processes that mask the expected long-distance variations (i.e., 550-m) of the catenary processes. Organic C, pH, bulk density, and soil moisture content showed various degrees of spatial continuity, but all indicated that the topographic/snow gradient is not the only dominant soil-forming factor in this alpine ecosystem. The estimated fractal dimension D for the grid landform and the mean snow depth varied between 1.2 and 1.4, indicating that they vary smoothly with long-range variation. The estimated D of the soil variables ranged between 1.6 and 1.8, showing a noisy appearance with short-range variations. These results strongly suggest that most small and micro-scale variations in the alpine soil environs resulted from the combined effect of cryoturbation, biological activity, parent-material and eolian deposition, whereas the large-scale variations originated as a result of the topographic/snow gradient.

Introduction

Numerous studies have suggested that topography is the most dominant geomorphic attribute of the alpine tundra ecosystem in the Colorado Front Range of the US Rocky mts. Along with strong westerly winds, topography controls the spatial gradient of snow accumulation and ablation, thereby dominating many of the biotic and abiotic processes along that gradient. For example, the topographic soil-forming factor creates a catena in which the soil moisture is highly correlated with the length of snow accumulation, and this, in turn, affects soil development (Burns and Tonkin 1982). The spatial variation of snow accumulation affects soil moisture (Taylor and Seastedt 1994), decay rates (O'Lear and Seastedt 1994), plant productivity (Walker et al. 1994), organic matter ac-

cumulation (Burns and Tonkin 1982), and CH₄ fluxes (West et al. 1999). It also governs the microbial processes, which control gross N mineralization and N immobilization among plant communities (Fisk et al. 1998).

Fisk et al. (1998) address the hypothesis that the topographic soil moisture gradient is the fundamental factor controlling the patterns of N turnover among plant communities and that the differences among plant species is considerably less important. Their emphasis on landscape patterns differs from other studies (e.g., Steltzer and Bowman (1998); Bowman and Conant (1994)), which suggest that plant species are quite important in controlling soil N transformation and may consequently influence plant community and ecosystem structure and function.

The above-cited literature suggests that the topographic/snow gradient, coupled with dominant plant species distribution, create significant variations in the biogeochemical processes controlling water, carbon, nitrogen, and trace gas flux. These processes function at various spatial scales; thus successful prediction of these processes requires quantitative analysis of the various spatial scales operating collectively in the alpine tundra soil milieu. Although most of the above-cited investigations generalize from their small-scale experimental plots to landscape scale, few have attempted to test this generalization (e.g., Walker et al. (1993)).

The objective of this study is to quantify the spatial structure of various observed ecosystem parameters (i.e., snow depth, slope, and topography) and soil variables (i.e., soil moisture, soil color variables, texture, bulk density, pH, and organic C), which control soil processes along the topographic/snow gradient. The quantification of the spatial structure will facilitate generalization from the experiment site to a regional scale and vice versa, and enable better selection of the optimal scale for soil and biogeochemical studies.

Research approach

The soil attributes that control nutrient availability in soils are organic matter content, soil moisture, pH, texture, sesquioxides content, and the type and amount of clay minerals. These parameters also affect the color variables (hue, value, and chroma) of the soil. Soil color can be used to predict other soil properties. For example, the value determined by the Munsell Color Chart is a good predictor of organic matter in soils of similar texture across a regional scale (Schulze et al. 1993). Soil color reflects the Fe oxide composition and content, which, in turn, affect the adsorption capacity of the soils with respect to oxyanions (Scheinost and Schwertmann 1999). The mathematical expression that describes a soil attribute as a function of a basic parameter, such as color, is defined as the pedotransfer function (PDF) (Bouma and van Lanen et al. 1987; Tietje and Tapkenhinrichs 1993). Because soil color variables are easily measured in the field, they can serve as excellent PDFs for quantification of various soil processes across different spatial scales.

Spatial models that describe soil processes on a soilscape or regional scale are based on the spatial arrangement and interconnectedness of soil parameters

(Webster and Oliver 1990). Geostatistical theory was developed for spatial interpolation between sampling points; it allows quantification of the optimal sampling strategy for the required accuracy and precision (McBratney and Webster 1983), determination of the spatial structure of soil attributes across the soilscape (Goovaerts and Chiang 1993), and construction of thematic maps that exhibit higher accuracy than general maps (Bregt et al. 1987). The use of PDFs in conjunction with geostatistical modeling has recently been suggested and their potential for addressing environmental problems has been strongly argued (Borough et al. 1994; Scheinost et al. 1997a, 1997b). Hence, the selection of soil color variables was made because they are easy and inexpensive to measure in large numbers, which provides a robust conditional cumulative distribution function (ccdf) for geostatistical modeling. Soil color variables may serve as PDFs for other soil characteristics (e.g., P sorption capacity) across the alpine soilscape.

Theory

Numerous researchers have demonstrated the efficacy of regionalized variable theory and the experimental variogram in describing spatial variation in soils (Cressie (1988); Isaaks and Srivastava (1989); Webster and Oliver (1990); Deutsch and Journel (1992), among many others). The experimental variogram describes the rate of change in a regionalized variable and measures the degree of spatial dependence between samples within geographical boundaries. The spatial structure of the regionalized variable can be described by the experimental variogram in the case of stationarity conditions. The experimental variogram splits the total variance of a data set into two parts. The first part represents the spatial variance between sample values relative to distance between samples. The second part represents local or random variance. Because the experimental variogram is a function of distance, the weights change according to the spatial arrangement of the samples (Isaaks and Srivastava 1989). By definition, the value of the theoretical variogram $\gamma(h)$ for a given distance h is the square of the expected difference (E) between the values of the samples separated by distance h :

$$\gamma(h) = E\{Z(x) - Z(x+h)\}^2 \quad (1)$$

where $Z(x)$ and $Z(x+h)$ are values of the regionalized variable at location x , and $x+h$ separated by the

vector h , known as the lag. The experimental variogram can be estimated from the data at hand by:

$$\gamma_i(h) = \frac{1}{2n(h)} \sum_{i=1}^{n(h)} [Z(x_i) - Z(x_i + h)]^2 \quad (2)$$

In addition to the traditional experimental variogram, other experimental measures of spatial continuity such as general relative semivariograms, pairwise relative semivariograms, and covariance function can be computed in isotropic and anisotropic modes. The general relative variogram is the traditional variogram as described in Equation (2), standardized by the square mean of the data used for each lag:

$$\gamma_{GR}(h) = \frac{\gamma(h)}{\left(\frac{m_{-h} + m_{+h}}{2}\right)^2} \quad (3)$$

where m_{-h} is the mean of $Z(x)$ values and m_{+h} is the mean of $Z(x + h)$ values. The pairwise relative variogram is computed by normalizing each pair of $Z(x)$ and $Z(x + h)$ by the squared average of the $Z(x)$ and $Z(x + h)$ values:

$$\gamma_{PR}(h) = \frac{1}{2N(h)} \sum_{i=1}^{N(h)} \frac{(Z(x) - Z(x + h))^2}{\left(\frac{Z(x) + Z(x + h)}{2}\right)^2} \quad (4)$$

The variograms described in Equation (3) and Equation (6) are particularly useful because they are resistant to data sparsity, and outliers, and can reveal spatial structure and anisotropy that could not be detected otherwise (Deutsch and Journel 1992). The covariance function is the traditional covariance commonly used in statistics:

$$C(h) = \frac{1}{N(h)} \sum_{i=1}^{N(h)} Z(x)Z(x + h) - m_{-h}m_{+h} \quad (5)$$

In addition to the semivariograms, a crossvariogram $\gamma_{ij}(h)$ that measures the spatial dependence between any pair of ecosystem or soil attributes can be computed:

$$\gamma_{ij}(h) = \frac{1}{2n(h)} \sum_{i=1}^{n(h)} [Z(x_i) - Z(x_i + h)][Y(x_i) - Y(x_i + h)] \quad (6)$$

An important property of the crossvariogram $\gamma_{ij}(h)$ is the ability to filter out the uncorrelated part of the nugget component, which may help to interpret the nugget effect on the simple semivariograms $\gamma_{ii}(h)$ and $\gamma_{jj}(h)$. Following Cressie (1988), the variable $Z(x_i)$ consists of a deterministic mean structure $\mu_i(x)$, called large-scale variation, and three zero-mean mutually independent, intrinsically stationary processes, called small-scale variation $\nu_i(x)$, micro-scale variation $\eta_i(x)$, and measurement error or noise $\epsilon_i(x)$:

$$Z(x_i) = \mu_i(x) + \nu_i(x) + \eta_i(x) + \epsilon_i(x) \quad (7)$$

In practice, it is impossible to distinguish between the micro-scale component and the measurement error component. The sum of the variances of $\eta_i(x)$ and $\epsilon_i(x)$ forms a discontinuity at the origin of the simple semivariogram, called the nugget effect. Equation (2) and Equation (6) can be rewritten to express the crossvariogram:

$$\gamma_{ij}(h) = \gamma\nu_i\nu_j(x) + \gamma\eta_i\eta_j(x) + \text{Cov}[\epsilon_i(x), \epsilon_j(x)] \quad (8)$$

where $\gamma\nu_i\nu_j(x)$ is the crossvariogram between $\nu_i(x)$ and $\nu_j(x)$. Assuming the measurement errors are independent (i.e., $\text{Cov}[\epsilon_i(x), \epsilon_j(x)] = 0$), the nugget effect on the crossvariogram $\gamma_{ij}(h)$ is due only to the covariance between micro-scale variations $\eta_i(x)$ and $\eta_j(x)$. If the contribution of measurement errors to the nugget effect observed on the simple semivariograms is great, a small nugget component on the crossvariogram is expected. On the other hand, a large nugget effect on the crossvariogram would suggest that the nugget effect on the simple semivariograms is due mainly to micro-scale variations common to the two variables. Because the micro-scale is smaller than the shortest sampling interval, a critical analysis of the semivariogram/crossvariogram nugget-effect structure can quantify the limiting scale effect of a given edaphic factor across the study site.

There are two additional typical features characteristics of experimental variograms and crossvariograms, namely range and sill. The range is the distance beyond which the variance value remains essentially constant, whereas the sill is the value where the variogram reaches a plateau. Another useful characteristic is the ratio of the nugget effect to the sill, which is commonly called relative nugget effect and is given in percentage.

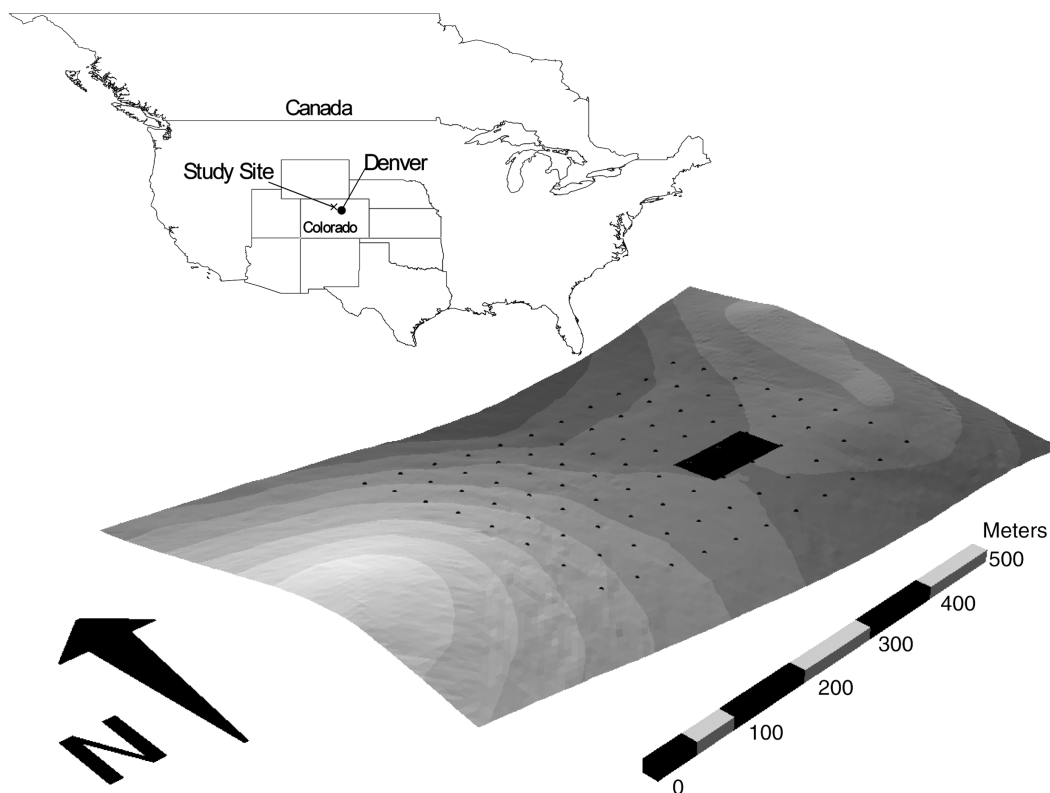


Figure 1. General location and 3-D drupe of the Saddle grid study area in Niwot Ridge, Front Range, Colorado, USA (40°03'N, 105°35' W). The black rectangle area represents the snow-fence grid location.

Material and methods

Field site

The study was conducted on Niwot Ridge, Front Range, Colorado, USA (Figure 1). Niwot Ridge has been a research site of the US Long-Term Ecological Research (LTER) program since 1980 and a site of the International Biological Program (IBP) in the 1970s. The study site is located in an area known as the Saddle, at an elevation of about 3525 m. A research grid of 17.5 ha (550 m × 400 m) wide that encompasses 70 50 × 50 quadrats marked by 88 stakes was established on the Saddle along a topographic/snow gradient (Walker et al. 1993). Soil development in Niwot Ridge was studied by Burns and Tonkin (1982) who formalized a synthetic alpine slope model to categorize micro-environmental sites across the alpine soilscape according to the edaphic-topographic-snow cover relationship. The most important site characteristic of this relationship was approximate snow-free days per year. For example, extremely windblown sites characterized by more than 300

snow-free days, wind blown sites by 225 – 300 days, minimal snow cover sites by 225 to 300 days, early-melting sites by 100–150 days, late-melting sites by 50–100 days, and wet meadow sites by ~ 100 days. Soil classification along the topography/snow gradient varied from Dystric Cryochrept in the wind blown site, Pergelic Cryumbrept in the minimal snow cover site, Typic Cryumbrept in the early snow melting site, Dystric Cryochrept in the late melting snow site, and various Cryaquepts and Cryaquolls in the wet meadow sites (Burns and Tonkin 1982). The plant association and species composition along this gradient has been fully described in Walker et al. (1993).

Multiple data sets have been collected at each grid point by various researchers since the 1970s, including snow depth, soil edaphic parameters, and plant species composition. Most of these data sets are available on the Web link to gopher archives (Ingersoll et al. 1997). The soil samples of the Saddle grid were collected in 1990 and analyzed for organic matter content, pH, bulk density, and moisture-content (gravimetric) and, using standard methods, by time-domain reflectometry (TDR). Soil texture was taken

from nodal plots (May and Webber 1982) across the Saddle in 1991 and was analyzed using the sieve-pipette method. The geographical patterns of the edaphic parameters across the Saddle grid or along vegetation nodal transect (May and Webber 1982) allowed meaningful spatial analysis. Other soil variables such as N and P content, were sampled only in clusters at a few locations that did not allow the construction of a meaningful cumulative conditional distribution function; hence they were not included in the spatial analysis.

The location and elevation of the 88 grid stakes, along with an additional 191 sampling locations, were geo-referenced using a Trimble Pathfinder ProXRS GPS unit with real time differential correction service. The horizontal accuracy of the real-time corrected GPS data is generally ± 1 m with a 95% confidence interval. The vertical accuracy of the GPS unit is ± 2 m with a 95% confidence interval. These geo-referenced points were input into Arc/Info GIS, which generated the digital elevation model (DEM) for the Saddle. The slope and aspect were calculated from the partial derivatives in the east-west and north-south directions, using the methodology and equations described by Frank (1988). We computed a slope-aspect index (SAI) relative to the prevailing westerly wind direction following the empirical relationships described by Frank (1988). We slightly modified Frank's SAI equation by not including the bit conversion constant in our computation. High values of SAI indicated areas that are generally leeward, snow-accumulation sites, whereas low SAI values indicated windblown, snow-free sites.

For the present study, color determination of soil samples was taken in the summer of 1999 at each grid point from depths of 0 to 5 cm and from 5 cm to 10 cm. The two-depth sampling scheme stemmed from our working hypothesis that the first sampling layer represents a soil horizon that is heavily influenced by eolian input (Litaor 1987a), whereas the second soil sampling layer better reflects the topographic/snow relationships in terms of soil moisture, parent-material, and catenary soil weathering. To test the influence of scale of sampling on the spatial continuity of the color PDF, we selected the snow-fence experiment site located in the middle of the topographic/snow gradient in the Saddle (Figure 1), where grid points were placed every 10 m on a 60 \times 70-m grid. The grid of the snow fence was installed across dry, moist, and wet-meadow communities, where the dominant plant species are the graminoid *Kobresia*

myosuroides, the forb *Acomastylis rossii*, and the graminoid *Deschampsia caespitosa*, respectively. The snow fence was installed in 1993 to simulate the effect of global climate change on the alpine ecosystem (Williams et al. 1998). The two-depth sampling scheme employed for the Saddle grid was also used for the snow-fence grid. For the purpose of the spatial analysis, the snow fence grid is part of the Saddle grid but with denser local measurements.

Each soil sample was air-dried and sieved through a 2-mm sieve. The soil color was identified using the Munsell Soil Color chart. Because successive pages of the soil color chart differ by 2.5 units of hue, visual color matching is somewhat less precise than measurement by reflectance spectra. Although the Munsell color system can be converted into a Cartesian system, it is less suited for multivariate statistical analyses, because hue and chroma do not represent Euclidean distances (Scheinost and Schwertmann 1999). Hence, the soil color of the soil samples was measured with a chroma meter (CR-310, Minolta Ossaka, Japan) using ground samples. The analysis was performed by lightly pressing the glass protection tube (CR-A33a) against a 5-mm thick layer of sample. The color was specified using the CIE- $L^*a^*b^*$ color system according to the recommendation of Melville and Atkinson (1985). The CIE- $L^*a^*b^*$ color system is defined as color coordinates where L^* measures the lightness of the sample; a^* measures redness when positive, gray when zero, and greenness when negative; and b^* values measure yellowness and gray when zero; and negative values indicate blueness. We also manipulated the CIE color coordinates to get a simple multiplicative redness index R_{Lab} ($R_{Lab} = a^*[a^{*2} + b^{*2}]^{0.5} \times 10^{10}/[b^*L^{*6}]$) described by Barron and Torrent (1986).

The precision and sample homogeneity (i.e., a measure of the amount of error in the data attributable to sampling technique) of the soil color determination were quantified by calculating the relative percent difference (RPD). The RPD is the quotient of the difference between field duplicates and the average of those results expressed as a percentage. Duplicate soil samples for color determination were collected from every 20 samples. The RPD for L^* , a^* , and b^* varied between 0.25% – 1.6%, 2.5% – 3.9%, and 4.7% – 7.6%, respectively. Laboratory triplicates of the color measurements varied between 0.01% and 0.09%. No RPD were calculated for the other soil attributes used in the present study, because no field duplicates or laboratory replicates were reported. However, experi-

ence shows that the RPD for most general soil variables, such as pH, OC, BD, soil moisture, and texture, varied between 30% and 15%.

The depth of the snow has been measured at 88 grid points on the Saddle from 1982 to 2000, which total more than 15,000 measurements. Depths were measured from fixed extendable poles on the western portion of the grid and by probing in the eastern part of the grid. Measurements during the winter months varied from once every two weeks to once a month, depending on the weather conditions. Measurements during the summer were performed biweekly until all snow disappeared or until snow accumulation began for the next winter. During the snow season of 1993, five replicates of snow-depth measurements in the vicinity of each grid point were taken to assess the within-grid-point variability. Measurements of snow depth were carried out to the nearest centimeter.

Geostatistical analyses

The geostatistical analysis was conducted using the algorithms and methodologies described by Deutsch and Journel (1992). The geostatistical modeling was performed in the following manner. First, a general exploratory data analysis was performed in which univariate statistics of the PDFs and the edaphic variables were obtained, and the benefits of data transformation was assessed. Next, if the general exploratory data analysis suggested that parametric spatial analysis was appropriate, then the experimental semi-variogram was computed. We used several variogram subroutines for each attribute under study, to ensure that the spatial variability/continuity measure was reproducible even when using various techniques. Each variogram was run in omnidirectional and directional modes and the variogram that exhibited the clearest structure (i.e., smallest nugget effect and best continuity) was selected. A minimum of 300 pairs of data points was used in the calculation of each lag class. The most common variograms used were the traditional variogram, general relative variogram, and the pairwise relative variogram. For the purpose of uniformity, we reported the variogram modeling results using the general relative variogram and traditional cross-variogram. The variogram modeling was performed using a trial-and-error approach as described by Deutsch and Journel (1992).

Results and discussion

Topographic/Snow gradient

The snow-depth data represented a repeated-measures design that had to be aggregated for the spatial analysis of the 88 georeferenced grid points. We selected two aggregation schemes that together best represent the spatio-temporal nature of the data. First, the data were averaged at each grid point using the entire monitoring period. Second, the data were aggregated at each grid point using the month of May of each year. The rationale for the aggregate scheme was the concept of the synthetic alpine slope (SAS) model (Burns and Tonkin 1982), which suggests that soil development across an alpine slope is controlled by the number of snow-free days per year, which, in turn, affects soil temperature and moisture (Table 1). The entire snow-depth aggregate scheme represents soil temperature better than it does moisture, because some of the snow that accumulated during the winter months was blown away or sublimated. The May snow depth is a good parameter for water equivalent, because it represents the maximum snowpack in spring, which determines the growing-season water budget for the plants. The moderate standard deviations (SD) around the means of both aggregates represent the cumulative effect of the spatio-temporal variations in these data sets. A smaller SD was observed in representative individual sites for the May snow-depth aggregate compared with the entire snow depth aggregate (Table 1), which suggests that the May snow-depth aggregate carries smaller temporal variations. The magnitude of the spatial variation within each grid point was tested using five repeated measures of snow depth taken within a 10 m radius around each stake. The results show that for most sites of the SAS model, the within point variance did not exceed 6% except for the extremely windblown and windblown sites (30% and 20% variation, respectively).

The spatial structure of the mean snow depth of both aggregate schemes exhibited a similar linear form, which can be easily extrapolated to its origin (Figures 2a, 2b). The apparent lack of a nugget effect suggests that within the 50 m grid spacing, there is little small-scale variability (< 50 m) of snow accumulation and melting. Similar results were obtained using other spatial continuity measures, such as covariance function, which showed very gradual change

Table 1. Summary statistics of snow-depth distribution on the Saddle grid.

Site†	Approx. snow-free days per year	Entire Data Set			May Snow-Depth			Entire Data Set (Representative Individual sites)			May Snow-Depth (Representative Individual sites)		
		X	SD	N	X	SD	N	X	SD	N	X	SD	N
EWB	> 300	15	14	(535)	23	18	(86)	15	11	(58)	25	16	(10)
WB	200 – 300	23	24	(1375)	36	27	(240)	24	21	(98)	46	29	(18)
MSC	150 – 200	124	92	(4754)	158	101	(855)	151	89	(124)	214	87	(19)
EMS	100 – 150	200	119	(2371)	294	106	(354)	203	111	(131)	323	80	(19)
LMS	50 – 100	250	132	(452)	363	110	(62)	288	137	(144)	411	95	(19)

† Site classification of Burns and Tonkin (1982). EWB = extremely wind blown, WB = wind blown, MSC = minimal snow cover, EMS = early melting snow bank, LMS = late melting snow bank & wet meadow.

in $C(h)$ near the origin, indicating strong spatial continuity.

The experimental variograms of both snow-depth aggregates exhibit strong spatial continuity across almost the entire grid distance of 500 m. The spatial dependence between the snow-depth and topoclimatic attributes, such as the slope aspect index (SAI), was tested using a crossvariogram modeling approach (Figure 2c). The spatial continuity of the crossvariogram clearly demonstrates the strong dependency of snow accumulation on the slope angle and its aspect in relation to the prevailing westerly winds. The small nugget effect of the crossvariogram confirms our earlier notion that minor and microscale variations in snow-depth accumulation across the Saddle grid were relatively small.

Soil color variables

The spatial structure of the soil color variables (L^* , a^* , b^* , and R_{Lab}) in the two sampling depths are depicted in Figures 3 and 4. The experimental variogram of the color variables in the top sampling depth exhibits a large relative nugget effect (nugget/sill = 46%) and a 300 m range of spatial dependency. The experimental variogram of the color variables in the deeper sampling depth (5 to 10 cm) exhibits a smaller relative nugget effect (30%) than the topsoil variogram and the spatial continuity extends across the entire grid area (Figure 4). The dissimilarity between these experimental variograms originates from the different soil processes operating at the two sampling depths. The topsoil horizon is significantly richer in dark organic matter, which obscured the redness index and resulted in considerable minor and microscale variations. The topsoil horizon is strongly affected by eolian deposition of organic matter and clay minerals (Litaor 1987a), which exhibit small varia-

tions upon falling on the snow but are redistributed along preferential flow paths during snowmelt. The redistribution of the eolian material created small and microscale variations, which somewhat reduced the spatial continuity of the color variables. Another potential source of the microscale variations in organic matter accumulation that may have obscured the redness index is plant species composition, which varied significantly across distances smaller than the grid spacing.

The soil color variables in the deeper sampling depth show strong correlation with both snow depth aggregates ($r = 0.75$, $P < 0.001$), in addition to spatial similarity in experimental variograms (see Figures 2a, 2b and 4). Parent-material in the Saddle varies greatly across the soilscape and it consists mainly of pre-Pleistocene glacial debris, mass wasting, and regolith (Mahaney and Fahey 1988) of various igneous and metamorphic rocks. Because of the large degree of heterogeneity observed in the parent-material across the Saddle and the continuous nature of the redness index, we suggest that the topographic/snow gradient is the dominant factor in catenary processes below the topsoil horizons. The catenary processes include the flux of infiltrating water from the snowmelt which, in turn, affects the weathering rates of common Fe-bearing minerals, such as augite and biotite, which are abundant in the deeper layer of these alpine soils (Litaor 1987b) and would create the observed continuum of the redness index.

The 50-meter interval of the Saddle grid was established somewhat arbitrarily, but it has been considered a reasonable research design for landscape scale (100 to 10⁶ m²) studies (Walker et al. 1993). The spatial analyses of the snow depth and soil-color attributes of the deeper horizon, using this grid size and spacing, demonstrate little discontinuity near the origin and smooth variography, which suggests that this

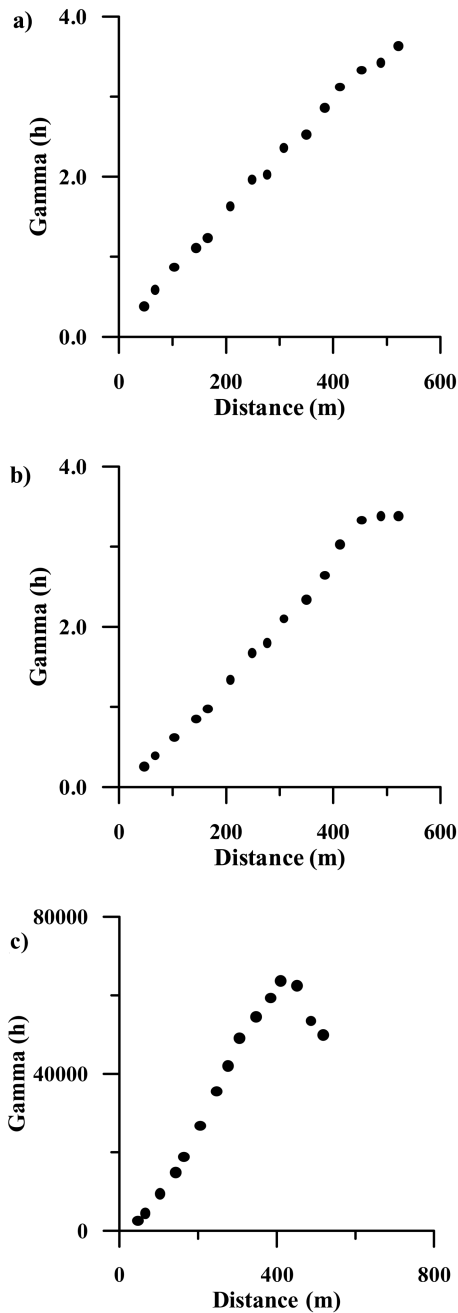


Figure 2. General relative omnidirectional variograms of the mean snow depth of a) the entire monitoring period b) and the spring snow depth aggregate and c) the traditional cross-variogram of snow depth and SAI across the topographic gradient in the Saddle. In the construction of these variograms and cross-variograms, we used 88 grid points, a unit separation of 35 m, with a lag tolerance of 18 m, and a bandwidth of 500 m.

grid spacing adequately covers large-scale variations. To further test this assessment, we used the snow-fence grid of 5 to 10 m sampling intervals to create a

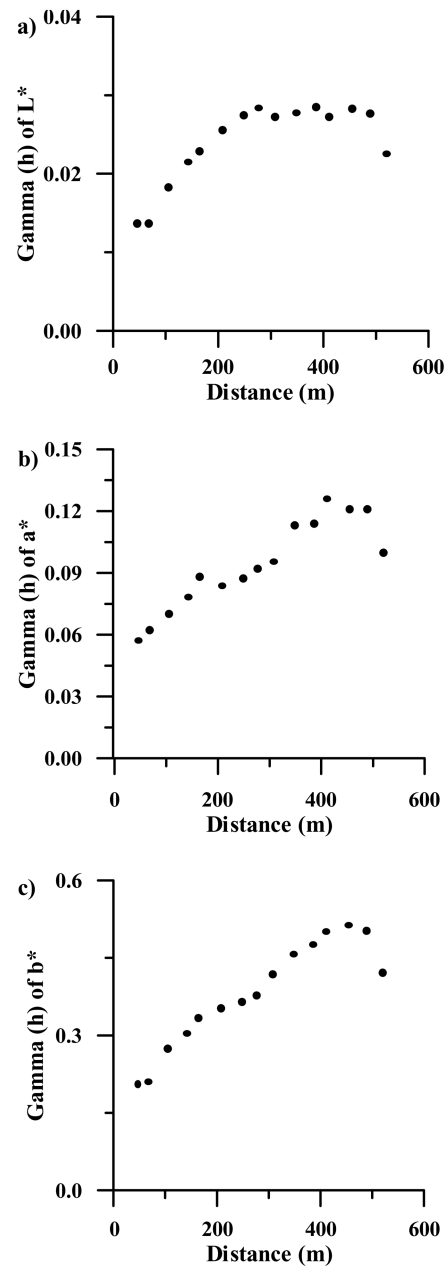


Figure 3. General relative omnidirectional variograms of the color variables (a) L^* , (b) a^* and (c) b^* in the topsoil sampling (0 – 5 cm) across the topographic gradient in the Saddle. The variogram modeling was done with 17 lags of 35-m separation distance, 18 m lag tolerance, and a bandwidth search of 500 m.

denser grid for the ccdf and construct variograms of the soil color variables under these sampling conditions (Figures 5 and 6). The results of the variograms for both sampling depths show that smaller spatial structures exist within the 50 m grid spacing. These findings suggest that nested sets of scale structure,

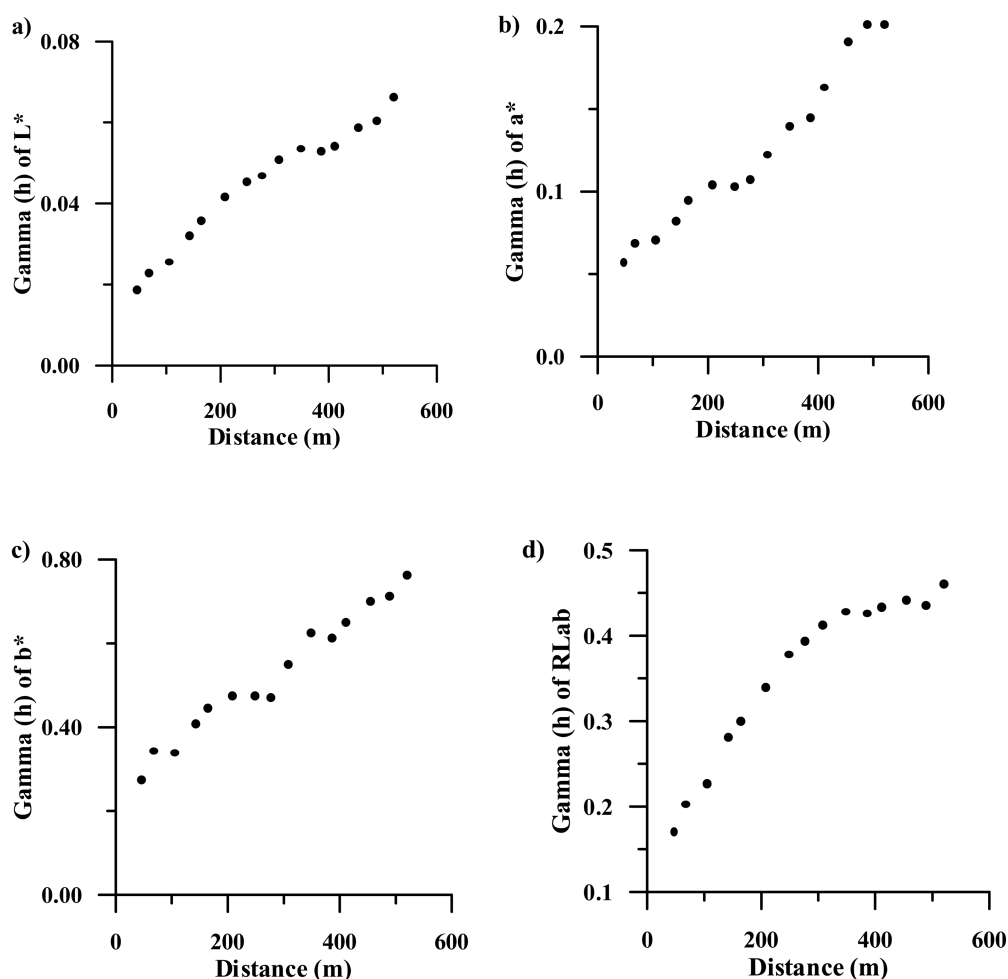


Figure 4. General relative omnidirectional variograms of the color variables (a) L^* , (b) a^* and (c) b^* and redness index (d) in the deeper soil sampling (5 – 10 cm) across the topographic gradient in the Saddle. The variogram modeling was done with 17 lags of 35-m separation distance, 18 m lag tolerance and a bandwidth search of 500 m.

known as the ‘gigogne effect’ (Burrough 1983), are operating in the alpine tundra of the Colorado Front Range. The snow-fence grid is located in the middle of the larger grid, where the slope change is negligible (0 to 2°) compared with the spatial change of plant species and community composition. Hence, the nested structures resulted from various soil-forming factors operating at different spatial scales of interaction.

General soil attributes

Six vegetation types defined by principal habitat and physiognomy (noda) have been identified in the Saddle (May and Webber 1982). Particle-size analyses were carried out in 30 of the nodal plots across the

alpine soilscape, whereas bulk density (BD) and soil moisture content were determined at each of the 88 grid points (Table 2). We constructed a directional variogram following the major direction of the nodal plots and omnidirectional variograms for bulk density (Figure 7). The spatial structure of the texture classes and bulk density shows almost a pure nugget effect, which entails a complete lack of spatial correlation. The weak correlation between the spatial structure of the texture classes and the topographic/snow gradient can be attributed to data sparsity, as well as other soil processes that mask the catenary processes.

The Saddle study site contains periglacial landforms that consist of turf-banked lobes and terraces, sorted polygons, strips, nets, debris islands, and earth hummocks and frost boils (Benedict 1992). The phys-

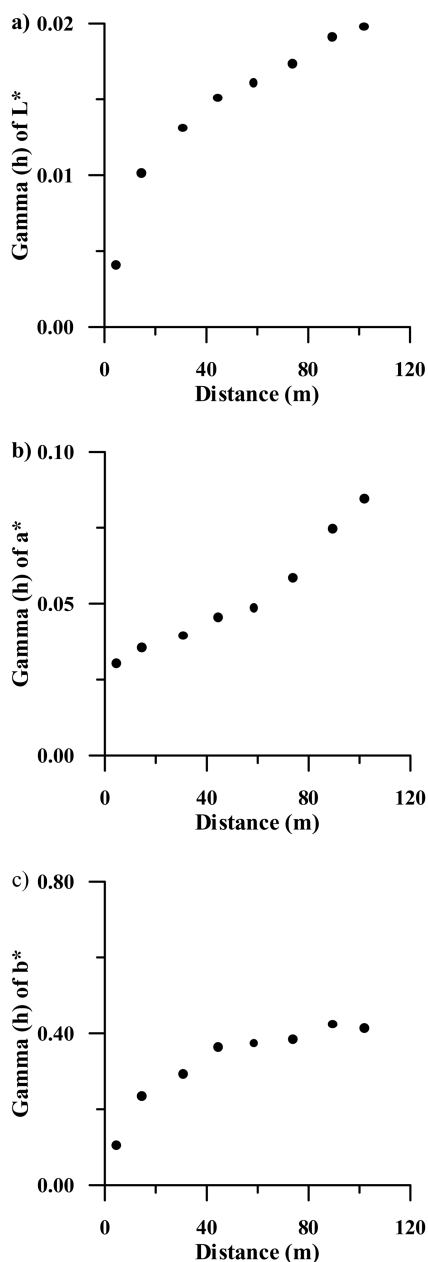


Figure 5. General relative omnidirectional variograms of the color variables (a) L^* , (b) a^* and (c) b^* in the topsoil sampling (0 – 5 cm) across the snow fence experiment gradient. The variogram modeling was done with 91 grid points, 9 lags of 15 m separation distance, 7 m lag tolerance, and a bandwidth search of 100 m.

ical process that dominates the formation of these periglacial landforms is upward intrusion of fine-textured mineral soil into the overlying humus-rich A and Oe horizons. Soil samples taken from a depth of 10 cm may contain particle-size classes originating from different sources, thus producing a more obscure

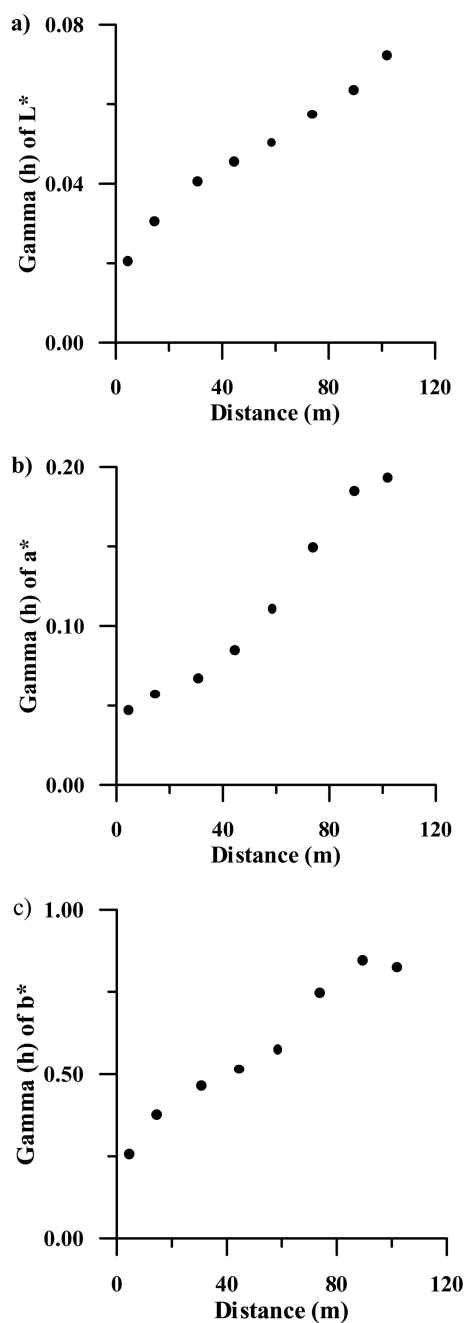


Figure 6. General relative omnidirectional variograms of the color variables (a) L^* , (b) a^* and (c) b^* in the deeper soil sampling (5 – 10 cm) across the snow fence experiment gradient. The variogram modeling was done with 91 grid points, 9 lags of 15 m separation distance, 7 m lag tolerance, and a bandwidth search of 100 m.

spatial structure than the a priori spatial model expected of catenary processes. Other soil processes may also contribute at various scales and obscure the catenary continuum. For example, pocket gophers'

Table 2. Summary statistics of selected soil attributes collected across the Saddle grid area.

Soil attribute		X	S.D.	Range
Bulk density	g cm ⁻³	0.88	0.2	0.4 – 1.6
Soil moisture	%	43.1	24.5	7.2 – 127†
Sand	%	59	12	30 – 83
Silt	%	23	6	10 – 34
Clay	%	17	6	5 – 37
pH		4.6	0.4	3.3 – 6.0
Organic C	g kg ⁻³	680	390	4 – 205

† Larger than 100% soil moisture content is commonly found in enriched organic horizons due to the hydrophobicity of organic matter.

activity homogenizes the soils in a highly spotty fashion (Litaor et al. 1996), creating a nested spatial structure that cannot be resolved using the current existing nodal plot sampling design. Other potential sources of minor and microscale variations that obscure the catenary interconnectedness are differential weathering of the Saddle regolith and preferential flow of snow-melt and soil interstitial waters.

The intrusion of fine-textured mineral soils to the rhizosphere due to cryoturbation resulted in soil material with higher clay and sesquioxide content, which control the specific-surface area, and, in turn, affect the availability of nutrients, especially phosphorus. Bowman et al. (1993) suggest that because of atmospheric N influx, phosphorus could become the limiting nutrient of the alpine ecosystem. Hence, future studies of the P cycle in this area should consider the nested spatial structures, which are a result of the various soil-forming factors and processes. One possible research approach for this problem is to use the soil-color variables as PDF for P sorption characteristics across the soilscape.

The experimental variogram of gravimetric soil moisture exhibits a large relative nugget effect (~ 50%) but with clear spatial dependency extending to a range of 400 m (Figure 8). The experimental variogram of soil moisture measured by the TDR exhibits almost a pure nugget effect for the first 400 m, followed by a very weak spatial dependency (Figure 8). The structural dissimilarity between the two variograms stems from their inherent differences in mode of measurements. The gravimetric soil moisture method incorporated composite samples collected around each grid point; thus it expunged small-scale variations, but retained the large-scale spatial dependency of soil moisture across the alpine soilscape. The TDR measures moisture along a narrow envelope

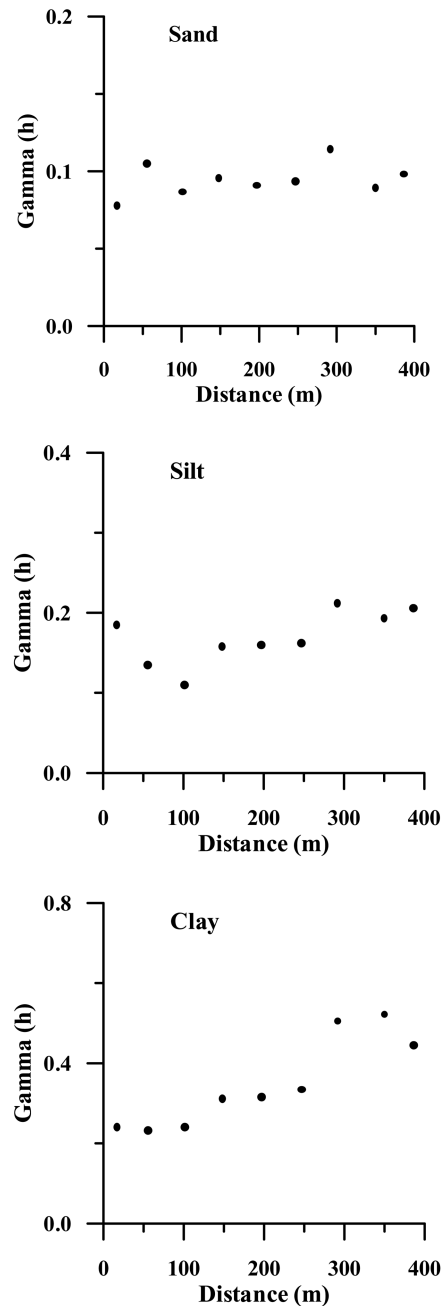


Figure 7. General relative directional variograms of sand, silt, and clay using 30 sampling nodal plots. The variogram construction was done with an azimuth of 155 degrees, 7 lags of 50 m separation distance, 25 m lag tolerance, and a bandwidth search of 500 m.

of soil around the vertical buried probes. In this mode of operation, the soil moisture is greatly affected by microenvironments, where the operational scale of measurement is only a few centimeters. Hence, using

the fixed locations of TDR measurements within the 50-meter grid resulted in an almost meaningless spatial model. To further test this notion, we measured soil moisture by taking 5 to 7 field replicates at separate locations within 1 m² at each of the 88 grid points of the Saddle, using a portable TDR (Trease, Soilmoisture Inc.). The coefficient of variations of the soil moisture at each of the 88 1 m² always exceeded 150% which is a strong indication for the influence of the micro-scale variations on the experimental variogram that cannot be resolved using the 50 m grid design.

The soil organic C and pH are important edaphic variables that control nutrient availability (e.g., N, P) and soil moisture. Their spatial analysis shows a clear structure with a moderate to large relative nugget effect (50–60%) and a continuity distance that varies between 200 and 400 m (Figure 9). The large relative nugget effect suggests that the spatial dependencies of organic C and pH are strongly affected by small and micro-scale variations. These variations may reflect the confounded effect of other soil-forming factors and processes such as biota, parent-material, and cryoturbation on the topographic/snow gradient. These variations operate at different spatial scales and, moreover, within each soil-forming factor and process, there are various spatial scales of interaction.

Fractal analysis

In order to further test the notion that the observed spatial variations originate from multiscale sources, we adapted the fractal approach described by Mandelbrot (1982) which was first adapted to nested spatial structures in soils by Burrough (1983). The level of variation present at all scales can be described by a single parameter, the fractal dimension D , defined by Mandelbrot (1982):

$$D = \frac{\log N}{\log r} \quad (9)$$

where N is the number of steps used to measure a pattern unit length and r is the scale ratio (for further discussion see Mandelbrot (1982)). The D values for a linear fractal curve can vary between 1 to 2. When D equals 1, it implies that a smooth curve can be fully approximated by a polynomial. When D is greater than 1, it implies that the line has a certain degree of fuzziness, which means uncertainty. If D equals 2, the

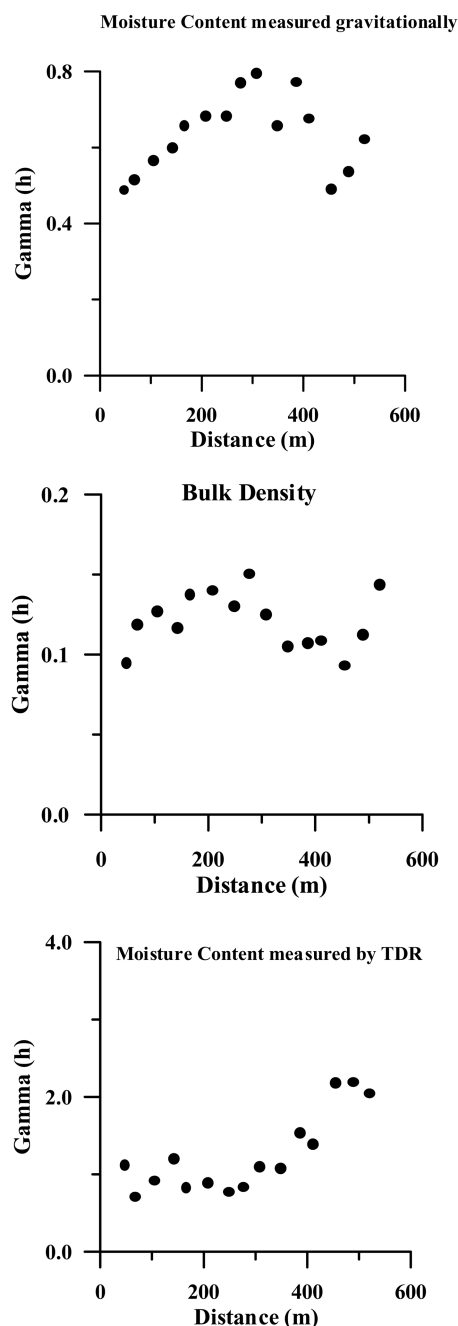


Figure 8. General relative omnidirectional variograms of bulk density and soil moisture content using 80 BD measurements and 41 TDR probes across the Saddle grid. The variogram construction was done with 10 lags of 35 m separation distance, 18 m lag tolerance, and a bandwidth search of 500 m.

fuzziness is so great that the linear fractal curve becomes crumpled. In practice, we estimated the D val-

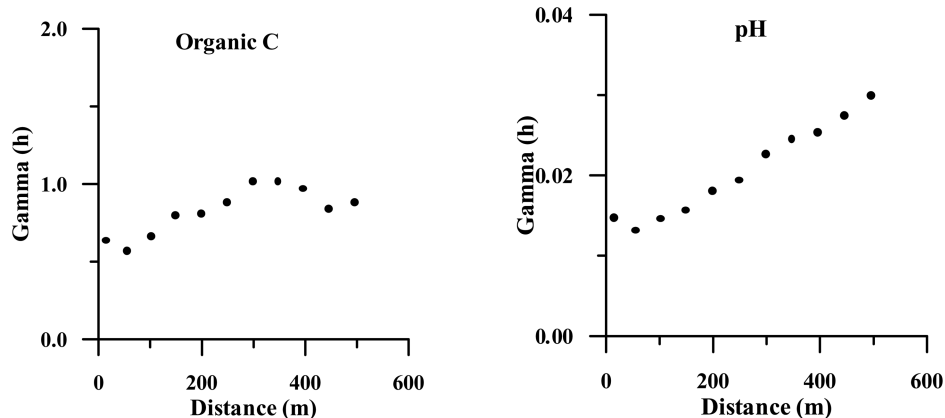


Figure 9. General relative omnidirectional variograms of organic C and pH content, using 110 measurements across the Saddle grid. The variogram construction was done with 10 lags of 35-meter separation distance, 18 meters lag tolerance, and a bandwidth search of 500 meters.

ues from the following relationships:

$$2\gamma(h) = h^{(4-2D)} \quad (10)$$

where h is the sampling interval and $\gamma(h)$ is the spatial structure. By plotting $\log\gamma(h)$ versus $\log(h)$, the slope of the line is equal to $4-2D$ (Burrough 1994).

In general, variation of landforms and water tend to have small D values, meaning that they vary smoothly with long-range variations. On the other hand, variations of soil variables are noisy, dominated by short-range variations (Table 3). These results confirm the expected range of D values. Topography and the mean snow depth show the smallest D values, whereas the soil properties exhibit larger values (Table 3). The low D values imply that the lag increments along the alpine grid tend to be positively correlated, whereas the high D values indicate that the lag increments along the sampling grid are negatively correlated with each other. This negative correlation means that the large positive increments that are usually followed by large negative increments give rise to wide short-term variation.

The small D value of the mean snow depth indicates the strong influence of topoclimatic factors, such as slope and aspect, on snow accumulation and melting, which resulted in large-scale variation, whereas local small-range variations have smaller effect on the spatial structure of these ecosystem attributes. The large D values of the alpine soil attributes strongly support our previous interpretation that the short-range variations observed in the variograms of most soil attributes are caused by the confounded effect of cryoturbation, biological action,

Table 3. Estimated D values for alpine attributes across the Saddle grid area.

Attribute	Lag (m)	D
Elevation	50	1.2
Mean Snow Depth	50	1.4
Organic C	35	1.7
pH	35	1.7
Bulk density	50	1.8
Soil Moisture Content	50	1.7
L^*	35	1.6
a^*	35	1.7
b^*	35	1.7
L^*	10	1.8
a^*	10	1.8
b^*	10	1.8

parent-material, and eolian deposition on the topographic/snow gradient that dominates the large-scale variations.

Conclusions

We studied the role of the topographic/snow gradient on soil processes in alpine tundra on Niwot Ridge of the Colorado Front Range by applying the regionalized variable theory and practice coupled with a fractal approach. The arbitrarily selected 50 m grid spacing installed in the 1970s was found adequate to describe the spatial dependency of snow accumulation on topoclimatic features, such as slope and aspect. Soil color variables measured at a sampling depth of 5–10 cm showed strong correlation with snow depth

and exhibited strong spatial continuity across the entire study area. These spatial relationships suggest that the large-scale variations observed in the soil color variables are strongly influenced by catenary processes. Soil color attributes measured in the top-soil horizon (0–5 cm) showed spatial distribution that consisted of large-scale as well as minor and micro-scale variations. Using a different grid size and spacing (10 m) to evaluate the discontinuity near the origin, clearly demonstrated that the soil color PDFs are best described by a nested structure, which was attributed to a confounded effect of various soil-forming factors on catenary processes. The spatial structure of texture classes exhibited no spatial structure and was explained by data sparsity, cryoturbation, and biological processes that mask the expected long-distance variations (i.e., 550-m) of the catenary processes. Organic C, pH, bulk density, and soil moisture content showed various degrees of spatial continuity but all indicated that the topographic/snow gradient is not the only dominating soil-forming factor in this alpine ecosystem. The estimated fractal dimension D for the grid landform and the mean snow depth varied between 1.2 and 1.4, indicating that they vary smoothly with large-scale variation. The estimated D of the soil variables ranged between 1.6 to 1.8, showing a noisy appearance with short-range variations. The fractal dimension results suggest that most short-range variations resulted from the combined effect of cryoturbation, biological activity, and parent-material and eolian deposition; whereas the large-scale variations originated from the topographic/snow gradient. Finally the spatial analysis results demonstrated the fuzzy and somewhat erratic nature of the soil attributes, which make the delineation of soil units boundaries difficult. Thematic soil maps in areas as complex as the Saddle site will undoubtedly carry large inherent uncertainty.

Acknowledgements

We would like to thank Mariah Carbone and Briana Constance for helping with the soil processing and color measurements. Partial support for this research was provided by Tel-Hai Academic College, Upper Galilee, Israel and by a U.S. National Science Foundation grant to the Long-Term Ecological Research (LTER) program at the University of Colorado. Data

used in this report are available online at <http://cult-er.colorado.edu:1030>.

References

- Barron V. and Torrent J. 1986. Use of the Kubelk-Munk theory to study the influence of iron oxides on soil color. *Jour. Soil Sci.* 37: 499–510.
- Benedict J.B. 1992. Field and laboratory studies of patterned ground in a Colorado alpine region. Occasional Paper No. 49. Institute of Arctic and Alpine Research, University of Colorado, Boulder, CO, USA, 38p.
- Bouma J. and van Lanen J.A.J. 1987. Transfer functions and thresholds values: From soil characteristics to land qualities. In: Bech K.J. (ed.), *Quantified Land Evaluation. Proc. Worksh. ISSS and SSSA, Washington, DC. 27 Apr.-2 May 1986.* Int. Inst. Aerospace Surv. Earth Sci. Publ. no. 6. ITC Publ., Enschede, the Netherlands, pp. 106–110.
- Bowman W.D., Theodose T.A., Schardt J.C. and Conant R.T. 1993. Constraints of nutrient availability on primary production in two alpine tundra communities. *Ecology* 74: 2085–2097.
- Bowman W.D. and Conant R.T. 1994. Shoot growth dynamics and photosynthetic response to increased nitrogen availability in the alpine willow *Salix glauca*. *Oecologia* 97: 93–99.
- Bregt A.K., Bouma J. and Jellinek M. 1987. Comparison of thematic maps derived from a soil map and from kriging point data. *Geoderma* 39: 281–291.
- Burns S.F. and Tonkin P.J. 1982. Soil-geomorphic models and the spatial distribution and development of alpine soils. In: Thorne C.E. (ed.), *Space and Time in Geomorphology.* Allen & Unwin, London, UK, pp. 25–43.
- Burrough P.A. 1994. Principles of Geographical Information Systems for Land Resources Assessment. Monographs on Soil and Resources Survey No 12. Oxford Science Publication, Clarendon Press, Oxford, UK.
- Burrough P.A., Bouma J. and Yates S.R. 1994. The state of the art in pedometrics. *Geoderma* 62: 311–326.
- Burrough P.A. 1983. Multiscale sources of spatial variation in soil. I. The application of fractal concepts to nested levels of soil variation. *Jour. Soil Sci.* 34: 577–597.
- Cressie N. 1988. Spatial prediction and ordinary kriging. *Math. Geol.* 20: 405–421.
- Deutsch C.V. and Journel A.G. 1992. *GSLIB-Geostatistical Software Library and User's Guide.* Oxford University Press, New York, 340p.
- Fisk M.C., Schmidt S.K. and Seastedt T.R. 1998. Topographic patterns of above- and belowground production and nitrogen cycling in alpine tundra. *Ecology* 79: 2253–2266.
- Frank T.D. 1988. Mapping dominant vegetation communities in the Colorado Rocky Mountain Range with LANDSAT thematic mapper and digital terrain data. *Photogrammetric Engineering and Remote Sensing* 54: 1727–1734.
- Goovaerts P. and Chiang C.N. 1993. Temporal persistence of spatial patterns for mineralizable nitrogen and selected soil properties. *Soil Sci. Soc. Am. J.* 57: 372–381.
- Ingersoll R.C., Seastedt T.R. and Hartman M.A. 1997. A Model Information Management System for Ecological Research. *BioScience* 47: 310–316.

- Isaaks E.H. and Srivastava M.R. 1989. *An Introduction to Applied Geostatistics*. Oxford University Press, New York, NY, USA, 561 p.
- Litaor M.I. 1987a. The influence of eolian dust on the genesis of alpine soils in the Front Range, Colorado. *Soil Science Society of America Journal* 51: 142–147.
- Litaor M.I. 1987b. Aluminum chemistry: fractionation, speciation, and mineral equilibria of soil interstitial waters of an alpine watershed, Front Range, Colorado. *Geochem. et Cosmochim. Acta*. 51: 1285–1295.
- Litaor M.I., Mancinelli R. and Halfpenny J. 1996. The influence of Pocket Gophers on the status of nutrients in alpine soils. *Geoderma* 70: 37–48.
- Mandelbrot B.B. 1982. *The Fractal Geometry of Nature*. Freeman, New York, NY, USA.
- May D.E. and Webber P.J. 1982. Spatial and temporal variation of the vegetation and its productivity on Niwot Ridge, Colorado. In: Halfpenny J.C. (ed.), *Ecological Studies in the Colorado Alpine*. Institute of Arctic and Alpine Research, University of Colorado, Boulder, CO, USA, pp. 35–62.
- Mahaney W.C. and Fahey B.D. 1988. Extractable Fe and Al in late Pleistocene and Holocene paleosols on Niwot Ridge, Colorado Front Range. *Catena* 15: 17–26.
- McBratney A.B. and Webster R. 1983. How many observations are needed for regional estimation of soil properties? *Soil Sci.* 135: 177–183.
- Melville M.D. and Atkinson G. 1985. Soil colour: its measurement and its designation in models of uniform colour space. *J Soil Sci.* 36: 495–512.
- O’Lear H.A. and Seastedt T.R. 1994. Landscape patterns of litter decomposition in alpine tundra. *Oecologia* 99: 95–101.
- Scheinost A.C. and Schwertmann U. 1999. Color identification of iron oxides and hydroxysulfates: Use and limitations. *Soil Sci. Soc. Am. J.* 63: 1463–1471.
- Scheinost A.C., Sinowski W. and Auerswald K. 1997a. Regionalization of soil buffering functions: A new concept applied to K/Ca exchange curves. *Advances in GeoEcology* 30: 23–38.
- Scheinost A.C., Sinowski W. and Auerswald K. 1997b. Regionalization of soil water retention curves in a highly variable soilscape, I. Developing a new pedotransfer function. *Geoderma* 78: 129–143.
- Schulze D.G., Van Scoyoc G.E., Henderson T.L., Baumgardner M.F., Negal J.L. and Stott D.E. 1993. Significance of organic matter in determining soil colors. In: Bigham and Ciolkosz (eds), *Soil Color*. SSSA Special Publication Number 31. Soil Science Society of America Inc., Madison, WI, USA, pp. 71–91.
- Steltzer H. and Bowman W.D. 1998. Differential influence of plant species on soil nitrogen transformations within moist meadow alpine tundra. *Ecosystems* 1: 464–474.
- Taylor R.V. and Seastedt T.R. 1994. Short- and long- term patterns of soil moisture in alpine tundra. *Arctic and alpine Research* 26: 14–20.
- Tietje O. and Tapkenhinrichs M. 1993. Evaluation of pedo-transfer function. *Soil Sci. Soc. Am. J.* 57: 1088–1095.
- Walker D.A., Krantz W.B., Price E.T., Lewis B.E. and Table R.D. 1994. Hierarchic studies of snow-ecosystem interactions: a 100 year snow alteration experiment. In: *Proceedings of the 50th Eastern Snow Conference*, pp. 407–414.
- Walker D.A., Halfpenny J.C., Walker M.D. and Wessman C.A. 1993. Long-term studies of snow-vegetation interactions. *BioScience* 43: 287–301.
- Webster R. and Oliver M.A. 1990. *Statistical Methods in Soil and Land Resource Survey*. Spatial Information System. Oxford University Press, New York, NY, USA, 316 p.
- West A.E., Brooks P.D., Fisk M.C., Smith L.K., Holland E.A., Jaeger C.H. et al. 1999. Landscape patterns of CH₄ fluxes in an alpine tundra ecosystem. *Biogeochemistry* 45: 243–264.
- Williams M.W., Brooks P.D. and Seastedt T. 1998. Nitrogen and carbon soil dynamics in response to climate change in a high-elevation ecosystem in the Rocky Mountains, USA. *Arctic and Alpine Research* 30: 26–30.